Title: Co-occurring genetic alterations in the RAS pathway promote resistance to MET inhibitor treatment in non-small cell lung cancer with a *MET* exon 14 skipping mutation

Authors: Julia K. Rotow[1,2], Philippe Gui[1,2], Wei Wu[1,2], Victoria M. Raymond[3], Richard B. Lanman[3], Frederic J. Kaye[4], Nir Peled[5], Ferran Fece de la Cruz[6], Brandon Nadres[6], Ryan B. Corcoran[6], Iwei Yeh[2,7], Boris C. Bastian[2,7], Petr Starostik[8], Kimberly Newsom[8], Victor R Olivas[1], Alexander M. Wolff[9], James S. Fraser[9], Eric A. Collisson[1,2], Caroline E. McCoach[1,2], Collin M. Blakely[1,2,10], and Trever G. Bivona[1,2,10]

[1]Department of Medicine, University of California, San Francisco, [2]Helen Diller Family Comprehensive Cancer Center, University of California, San Francisco, [3]Guardant Health, Inc, [4]Department of Medicine, University of Florida, [5]Soroka Medical Center, Ben-Gurion University, Beer-Sheva, Israel [6]Massachusetts General Hospital Cancer Center and Department of Medicine, Harvard Medical School, [7]Departments of Dermatology and Pathology, and Clinical Cancer Genomic Laboratory, University of California, San Francisco, [8]Department of Pathology Immunology and Laboratory Medicine, University of Florida, [9]Department of Bioengineering and Therapeutic Sciences, University of California, San Francisco, [10]Co-corresponding authors.

Abstract:

While patients with advanced-stage non-small cell lung cancers (NSCLCs) harboring *MET* exon 14 skipping mutations (*MET*ex14) often benefit from MET tyrosine kinase inhibitor (TKI) treatment, their long-term survival is limited by drug resistance. The molecular basis for this resistance remains incompletely understood. Through targeted sequencing analysis of cell-free circulating tumor DNA obtained from 289 patients with advanced-stage *MET*ex14 NSCLC, we find prominent co-occurring *RAS* pathway gene alterations (e.g. in *KRAS/NRAS*, *NF1*). Clinical resistance to MET TKI treatment was associated with the presence of these co-occurring alterations. In a new preclinical model expressing a *MET*ex14 mutation, KRAS overexpression promoted MET TKI resistance, which was overcome by co-treatment with crizotinib and the MEK inhibitor trametinib. Our study provides a genetic landscape of co-occurring alterations in advanced-stage *MET*ex14-mutated NSCLC and suggests a potential combination therapy strategy to enhance clinical outcomes.

Statement of Significance:

This report describes targeted sequencing of the largest reported cohort of advanced-stage NSCLC with a *MET* exon 14 skipping mutation. The data uncover certain RAS pathway genetic alterations as potential mediators of MEK TKI resistance, which could be overcome by MEK and MET co-inhibition in NSCLC.

Introduction:

Somatic mutations near splice sites in *MET* lead to splicing-mediated loss of exon 14, and a stabilized and possibly hyperactive MET protein. These *MET*ex14 mutations are an emerging therapeutic target in NSCLC and play a driver role in 2-4% of lung adenocarcinomas (1,2). MET tyrosine kinase inhibitor (TKI) treatment was associated with improved overall survival in a retrospective study of patients with *MET*ex14 NSCLC. (3). Response rates to treatment with the multi-kinase inhibitor crizotinib, which has activity against MET, were as high as 68% in a phase I clinical trial (3,4), with a progression free survival of 7.3 months in one case series (5).

Both intrinsic and acquired resistance limit the long-term survival of patients with *MET*ex14 NSCLC. Second-site *MET* mutations occur at acquired resistance in these patients after an initially favorable response to MET TKI treatment. These mutations include the second-site *MET* Y1230C/H/S, D1228A/H/N, and G1163R mutations at residues critical for type I MET TKI binding (e.g. crizotinib), against which type II MET TKIs may retain activity (6-8). Activation of downstream and parallel signaling pathways can bypass inhibition of the primary oncogenic driver in other NSCLC genetic subtypes (e.g. *EGFR*-mutant, *ALK* rearrangement positive), comprising a second main class of resistance mechanisms (9). While the signaling pathways downstream of activated MET include the RAS-RAF-MAPK and PI3K pathways (10), their role in targeted therapy resistance is not well-understood, and potential bypass track-based resistance mechanisms have yet to be reported in *MET*ex14 NSCLC.

Recent studies show that advanced-stage NSCLCs often harbor multiple oncogenic alterations that may impact therapeutic response (11-13). A more detailed understanding of the mutational landscape which co-exists with oncogenic *MET* alterations in NSCLC, including amongst these parallel and bypass signaling pathways, may facilitate an improved understanding of MET TKI

resistance determinants and identify rational polytherapy strategies to improve clinical outcomes. Analysis of cell-free circulating tumor DNA (cfDNA) provides one avenue to describe the genomic landscape within a tumor and offers the potential to capture genomic changes reflecting heterogeneity across distinct metastatic tumor sites (11,14).

Here, we describe the spectrum of co-occurring genomic alterations observed within cfDNA of patients with *MET*ex14-harboring, advanced-stage NSCLC and identify prominent alteration of RAS pathway genes, including *KRAS*, in association with MET TKI resistance.

Results:

Co-occurring genomic alterations are common in advanced-stage METex14 mutated lung cancer

We studied a cohort of 289 patients with advanced-stage NSCLC with a *MET*ex14 mutation identified upon cfDNA analysis of 68 cancer-relevant genes using a clinically validated assay, to evaluate the frequency with which *MET*ex14 mutations co-occur with other cancer-associated mutations (Supplemental Table S1) (11,15). Synonymous mutations and those with predicted neutral or unknown functional impact were excluded as previously described (11), as were mutations previously associated with clonal hematopoiesis (16). 86.5% of samples contained co-occurring genomic alterations, with a mean of 2.74 alterations per sample (range 0-22) in addition to the *MET*ex14 mutation. The most commonly altered genes, co-occurring with the *MET*ex14 mutation in at least 10% of patients, were *TP53* (49.5% of patients), *EGFR* (16.3%), *NF1* (15.6%), *BRAF* (10.7%), and *CDK4* (10.4%) (Figure 1A). Additional *MET* gene alterations were also common in this patient population, in which 9.3% of patients had co-occurring *MET* copy number gain and 12.5% had a co-occurring second-site *MET* mutation (Figure 1A). Including all identified *MET* second-site mutations, regardless of predicted functional impact, 17 of 34 mutations were located in the tyrosine kinase domain. Of these, fourteen (G1163R, L1195V/F, F1200I, D1228H/N/Y, and Y1230H/S) were located at residues previously associated with MET TKI resistance (6-8,17-19). Nine of these occurred in patients with known prior MET TKI exposure and five in patients with unknown prior treatment history. The remaining three mutations (H1094Y, R1336W, and I1084L) occurred in patients without available prior treatment history. While the *MET* H1094Y mutation is known to lead to MET activation (20), the other two mutations remain uncharacterized.

The co-occurrence of other established oncogenic driver alterations (*KRAS, EGFR, ALK, ROS-1, BRAF*) was uncommon except for the presence of activating *KRAS* mutations in 5.2% of patients (G12C/D/S/V 3.5%, G13C 1%, Q22K 0.3%, and Q61H 0.3%), canonical *EGFR*-activating mutations in 3.5% (del19 3.1%, L858R 0.7%, T790M 2%), and an *ALK* fusion in 0.7%. In addition, a *HER2* exon 20 insertion was detected in one patient. In a patient with known clinical outcomes data, with both *EGFR* del19/EGFR T790M mutations and a *METex*14 mutation, there was partial response (RECIST 1.1) to second-line treatment with the EGFR TKI osimertinib, which was ongoing at 11 months treatment.

The spectrum of co-occurring gene alterations differs between NSCLCs with a MET exon 14 skipping mutation or an activating EGFR mutation

To understand how the genomic landscape in advanced-stage *MET*ex14 NSCLC compares to NSCLCs with a different targetable oncogenic driver mutation, we used identical cfDNA profiling to compare a cohort of patients with known *MET*ex14 NSCLC to a separate, stage-matched cohort of 1653 samples from 1489 patients with advanced-stage *EGFR*-mutant (del19, L858R)

NSCLC (Supplemental Table S1) with identical filters to remove mutations with predicted unknown or absent function impact and mutations previously associated with clonal hematopoiesis. This comparison demonstrated differential frequency of co-occurring genomic alterations in 17 genes (Figure 1B). In the *MET*ex14 cohort, *NF1*, *CDK4, STK11*, *ALK, KRAS*, *ATM*, *CDKN2A*, *NRAS, TSC1*, and *ESR 1* were more commonly identified. In the *EGFR*-mutated cohort, co-occurring alterations in *AR, ERBB2*, *CCNE1*, *PIK3CA, BRAF*, *CTNNB1,* and *MYC* were more commonly identified, consistent with our prior findings identifying these as common co-occurring alterations in *EGFR*-mutant NSCLC (11). Among the 10 genes with a greater frequency of genomic alteration in patients with a *MET*ex14 mutation, three (*NF1*, *KRAS*, and *NRAS*) were involved in the RAS-RAF-MAPK signaling pathway.

Both MET second-site mutations and gene alterations promoting bypass pathway activation are acquired following MET TKI exposure

We identified twelve patients with cfDNA obtained following treatment with crizotinib, with an available matched comparator sample obtained prior to known crizotinib exposure (Table 1, Supplemental Table S2). A potential mechanism of resistance to MET TKI therapy was identified in all but four patients, including both on-target resistance via *MET* second-site mutations and activating changes in potential parallel signaling pathways. Details regarding one patient (patient 5) in this dataset have previously been published by other groups (6,8).

MET second-site mutations (Y1230H/S, D1228H/N, F1200I, L1195V) were seen in four of twelve patients (Table 1, Supplemental Table S2). With the exception of the *MET* F1200I mutation, these second-site mutations have been reported in patients with acquired MET TKI resistance (6-8,17-19). Like the *MET* L1195V mutation, in preclinical studies the *MET* F1200I mutation is predicted to alter the kinase domain conformation such that it interferes with the binding of type II MET TKIs within the DFG-out binding pocket, and to a lesser extent to interfere with type I MET TKI effect through loss of an autoinhibitory MET conformation (Supplemental Figure S1) (6).

Potential parallel and downstream pathway alterations were found in 7 patients (Table 1). These included an activating *KRAS* mutation and *KRAS* copy number gain (Figures 2A and 2B). Also within the RAS pathway, an *NF1* frameshift mutation (NF1 p.Gln2636fs) was found in one patient. Loss of function mutations in *NF1* lead to RAS/RAF/MAPK pathway hyperactivation and are a potential therapeutic target for MEK inhibition in NSCLC (NCT03232892) (9). Copy number gain of the receptor tyrosine kinases *EGFR* and *KIT* that act upstream of the RAS pathway were present in four patients. Both *KIT* and *EGFR* encode receptor tyrosine kinases capable of providing alternative oncogenic signaling through, in part, RAS/RAF/MAPK activation, and are implicated in resistance to crizotinib in *ALK*-rearranged NSCLC (21), but have not been described in the *MET*ex14-mutated setting.

Emergence of RAS pathway genetic activation during MET TKI resistance

We identified a patient within the described cfDNA cohort on whom serial plasma cfDNA analysis was performed during treatment with a MET TKI (Figure 2A, patient one in Table 1). The patient was an 84 year-old male with a 30 pack-year history of tobacco use and presented with metastatic pulmonary adenocarcinoma involving the lungs, lymph nodes, axial skeleton, and brain. While there was insufficient tissue upon diagnostic tumor biopsy for molecular testing, evaluation of plasma cfDNA using the Guardant360® clinical assay identified a canonical *MET*ex14 skipping mutation (c.3028+3A>G; variant allele frequency 7.6%). The patient received stereotactic radiosurgery to brain lesions, followed by the MET TKI crizotinib at 250 mg twice daily. After four weeks treatment repeat imaging demonstrated a radiographic partial response (RECIST 1.1) with

a decrease in *MET*ex14 cfDNA variant allele frequency (VAF) to an undetectable level. Crizotinib was subsequently dose-reduced and then held for treatment-associated fluid retention, which was followed by radiographic disease progression and a return of the *MET*ex14 variant to levels detectable in plasma within four weeks (Figure 2A, Supplemental Table S3). Progression continued despite return to full dose crizotinib treatment.

Targeted sequencing of 479 cancer-associated genes using the UCSF500 next generation sequencing (NGS) assay (22) was performed on a tumor biopsy of a progressing metastatic soft tissue rib lesion and identified a high level wild-type *KRAS* copy number gain (~22x fold), in addition to other genetic variants of unknown significance (Supplemental Table S4) and the known *MET*ex14 skipping mutation. The UCSF500 assay utilizes control sequencing of peripheral blood mononuclear cells, which allows for more precise identification of somatic variants and reduces risk of false positive results related to detection of genomic alterations associated with clonal hematopoiesis. Serial cfDNA analysis also showed wild-type *KRAS* copy number gain in a sample obtained 8 weeks after this biopsy, followed by emergence of the *MET* Y1230S and F1200I mutations on subsequent samples. (Figure 2A, Supplemental Table S3). Pathology review of the progressing rib lesion biopsy sample confirmed persistent adenocarcinoma histology, without evidence of histologic transformations (Supplemental Figure S2). The FDA-approved MEK inhibitor trametinib (2 mg daily) was added to crizotinib (250 mg twice a day) in an attempt to target the activity of the downstream high level *KRAS* copy number gain that was hypothesized to drive MEK TKI resistance in this patient. A molecular response was observed after two weeks of combined trametinib and crizotinib treatment, with decrease in the cfDNA VAF of all identified *MET* mutations and return to undetectable *KRAS* copy number gain (Figure 2A, Supplemental Table S3). However, the patient continued to decline clinically with fatigue, fluid retention, and diarrhea consistent with toxicity of the combination therapy regimen despite dose-reduction of trametinib to 2 mg every other day, and expired before radiographic response could be assessed.

KRAS amplification and KRAS G12D mutation upon MET TKI resistance

A second patient was identified with a canonical *MET* exon 14 skipping mutation and acquired KRAS gene alterations in the setting of crizotinib resistance (Figure 2B, patient two in Table 1). This 67 year-old male without a history of tobacco use was diagnosed with pulmonary adenocarcinoma metastatic to the adrenal gland. Targeted sequencing of a dominant right upper lobe lung lesion demonstrated a *METex14* mutation (2888-19_2895del27), with wild-type *KRAS (*Figure 2B, Supplemental Table S5*)*. Plasma cfDNA testing using the FoundationACT® clinical assay demonstrated the known *MET*ex14 mutation and an activating *KRAS* G12D mutation (Supplemental Table S5). He was treated with crizotinib in the first-line setting with a mixed tumor response after two months. While the biopsied right upper lobe pulmonary lesion responded to treatment (RECIST 1.1), a second smaller right upper lobe pulmonary lesion and an adrenal lesion enlarged, consistent with primary MET TKI resistance (Figure 2B). Confirmatory droplet digital PCR (ddPCR) testing verified absence of the *KRAS* G12D mutation within the pre-treatment biopsy sample to a sensitivity of <0.02%, while confirming the presence of the known *METex14* mutation (present in 11% of alleles).

Following stereotactic body radiotherapy (SBRT) to the progressing lung and adrenal lesions, the patient continued to receive crizotinib with radiographic response until 7 months of treatment, when a progressing abdominal lesion adjacent to the prior adrenal lesion and progressing lung nodules were detected. A biopsy of the progressing abdominal lesion identified the known *MET*ex14 mutation (77.9% VAF) and *KRAS* G12D mutations (47.4% VAF), and also found *KRAS* copy number gain (~11-fold), along with other gene alterations of less certain significance

(Supplemental Table S5). Next-generation DNA sequencing of the patient's peripheral blood mononuclear cells (PBMCs) confirmed absence of detectable *KRAS* G12D mutation within the hematopoietic lineage. He was subsequently treated with platinum-based chemotherapy with radiographic response.

KRAS overexpression induces resistance to crizotinib that is overcome by co-treatment with trametinib

The clinical data suggested that hyperactivation of certain RAS pathway genes (e.g. *KRAS*) may induce resistance to MEK TKI treatment in *MET*ex14 NSCLC. We engineered a new Ba/F3 cell-based system to assess the impact of RAS pathway hyperactivation on sensitivity to MET TKI treatment. The IL-3 dependent Ba/F3 cell line, while not of epithelial origin, is an established system to assess oncogenic capacity and putative drug resistance mechanisms (23,24). Stable expression of human *MET*ex14 within the Ba/F3 cell line in the presence of the MET ligand human HGF induced IL-3 independent growth, to a greater extent than stable expression of wild type MET (Figure 3A). Increased downstream Erk phosphorylation was observed with *MET*ex14 versus wild type *MET* (Supplemental Figure S3). IL-3 independent growth was not seen in the absence of HGF treatment (Figure 3B), consistent with the known functional consequences of *MET*ex14 skipping, which leads to reduced MET degradation but not necessarily to ligand-independent MET activation (25).

*MET*ex14 expressing cells were sensitive to treatment with crizotinib, as measured by reduced cell growth on cell viability assays (Figure 3C), and decreased Erk phosphorylation was observed upon crizotinib treatment with associated increase in cleaved PARP indicative of apoptosis (Supplemental Figure S3). To model the clinical cases, we then tested whether the forced overexpression of wild type KRAS (to mimic copy number gain or mutational activation) in *MET*ex14-expressing cells had an effect on response to crizotinib. We generated KRAS-overexpressing cells in the *MET*ex14 background and performed viability experiments, which showed that the cells became resistant to single-agent MET TKI treatment, with an increase in IC50 to crizotinib (IC50 of 0.16 μM in control cells versus 1.68 μM in KRAS overexpressing cells, *p*-value < 0.001) (Figures 3C and 3E). We then treated these cells that harbor both *MET*ex14 and KRAS overexpression with a combination of crizotinib and trametinib in order to block both MET signaling and downstream MAPK pathway signaling. METex14-expressing cells overexpressing KRAS were re-sensitized to MET inhibition when co-treated with the MEK inhibitor trametinib (crizotinib IC50 of 1.68 μM in the absence of trametinib versus 0.25 μM with trametinib co-treatment, *p*-value < 0.001) (Figure 3D and 3E). The selected trametinib dose reduced but did not eliminate cell growth in the absence of crizotinib (Supplemental Figure S4). Immunoblot analysis demonstrated Erk phosphorylation despite crizotinib treatment in samples with *KRAS* overexpression, which was abrogated by the addition of trametinib. The combination treatment was associated with increased cleaved PARP indicative of tumor cell apoptosis (Supplemental Figure S3). Overall, these results show that *MET*ex14 expression confers oncogene addiction in the presence of HGF. These cells are sensitive to MET inhibition and are rescued by RAS pathway hyperactivation via KRAS overexpression. Combination treatment with both MET and MEK inhibitors overcomes MET TKI resistance induced by KRAS overexpression in this system.

Discussion:

The challenge of therapeutic resistance is emerging as a key problem in the management of patients harboring *MET*ex14 mutations as they increasingly receive treatment with MET-targeted

therapies. Downstream and bypass oncogenic signaling pathway activation cause therapeutic resistance to TKIs in cancers with other oncogenic drivers (9), but such mechanisms have not previously been described in *MET*ex14 NSCLC, in which second-site mutations in *MET* itself have taken center stage to date. We found that alterations (mutation or amplification) of certain RAS/RAF/MAPK pathway genes including *NF1, KRAS,* and *NRAS* alterations are enriched in *MET*ex14 NSCLC compared to NSCLCs with canonical *EGFR*-activating mutations, using a large, consecutively collected cfDNA clinical cohort described here. We additionally identify patients with *MET*ex14 NSCLC demonstrating RAS pathway co-alterations including *KRAS* mutation or copy number gain during MET TKI resistance, that were present upon both plasma cfDNA analysis and tumor-based DNA sequencing. This is a novel description of downstream MAPK pathway activation at resistance to MET TKI therapy, consistent with established roles of MAPK pathway hyperactivation in promoting resistance to EGFR, ALK, BRAF, and ROS1 targeted therapies via diverse mechanisms including *KRAS* amplification and *KRAS, BRAF*, and *NF1* mutations (26-34).

The presence of acquired co-occurring downstream or bypass pathway alterations (e.g. *KRAS* copy number gain or mutation) may identify patients who will benefit from pathway-targeted rational polytherapy strategies. In our *MET*ex14 preclinical model system, KRAS overexpression induced MET TKI resistance that was overcome by the addition of the MEK inhibitor. The patient presented here who was similarly treated with this combination therapy showed evidence of molecular response but unfortunately experienced excess adverse effects when receiving this treatment. Though MEK inhibition was ineffective as treatment for activating *KRAS* mutations in the phase III SELECT-1 trial (35), the potential for activity against tumors bearing other genomic alterations leading to MAPK pathway activation, such as *KRAS* amplification or *NF1* loss of function mutations warrant investigation. Future efforts to combine these agents will require attention to agent selection and dosing for tolerability and efficacy.

The plasma cfDNA analysis presented here from a large cohort of patients with *MET*ex14 NSCLC demonstrates co-occurring genomic alterations in the majority of samples, reminiscent of recent studies in patients with *EGFR*-mutated NSCLC and consistent with a smaller cohort of 13 patients previously described with advanced-stage *MET*ex14 NSCLC (11,36). While plasma cfDNA-based testing provides a minimally invasive tool to query the tumor genomic landscape and offers the potential to capture heterogeneity across multiple tumor sites, recent reports have highlighted the challenge of false positive tumor tissue or plasma cfDNA testing due to detection of gene alterations deriving from incorporation of hematopoietic cells undergoing clonal expansion (16,37). To account for this issue, we excluded 866 variants in 206 genes previously associated with clonal hematopoiesis (16) from our reported cfDNA cohort. Additionally, in the described cases with *KRAS* genetic alterations at MET TKI resistance, PBMC sequencing reduced the probability of clonal hematopoiesis as the origin of the described KRAS variants.

Clinically, while many *MET* second-site mutations acquired during type I MET TKI (e.g. crizotinib) treatment may be overcome by use of type II MET TKIs (e.g. cabozantinib) (6-8), the bypass pathway resistance mechanisms described here will likely require a different therapeutic strategy, such as pathway-targeted combination therapy. Overall, this study enhances the understanding of the role of co-occurring genetic alterations in *MET*ex14-mutated NSCLC, with implications for the improved molecular diagnosis, serial monitoring of resistance mechanisms during treatment, and development of new rational therapeutic strategies to combat MET TKI resistance and enhance clinical outcomes.

Methods:

Patients: Patient samples were obtained and analyzed in accordance with IRB-approved protocols. The cfDNA analysis included 332 consecutive samples from 289 patients with advanced (stage IIIB/IV) non-small cell lung cancer with a *MET*ex14 mutation obtained between October 2015 and March 2018, and 1653 consecutively tested samples from 1489 patients with *EGFR*-mutated NSCLC (L858R and del19) obtained between April 2016 and May 2017.

Cell lines and reagents: Ba/F3 cells were purchased from ATCC (ATCC® HB-283™) and maintained in culture for a total of approximately 2-3 months in DMEM supplemented with 1 ng/mL IL-3 (Peprotech). Mycoplasma testing was not performed. Retrovirus was generated using TransIT-LT1 transfection reagent (Mirus). Cells were infected with filtered retrovirus, expressing either mCherry, human MET^{WT} or human MET^{ex14} in a pBABE-puro vector backbone as previously described (8) and selected in puromycin (2 µg/mL). Expression was confirmed by immunoblotting. KRAS-overexpressing cells were obtained by retroviral infection with a pBABE-hygro *KRAS4B* construct and selected in hygromycin (800 µg/mL). All drugs were purchased from Selleck Chemicals.

Transformation and cell proliferation assays: Transformation assay was performed by removing IL-3 through centrifugation and adding 50 ng/mL human HGF (Peprotech 100-39H). For proliferation assays cells were seeded in 96-well plates at 5,000 cells/well and the following day were exposed to crizotinib (Selleck Chemicals, #S1068) at 0 to 10 µM and/or trametinib (Selleck Chemicals, #S2673) at 0.01 µM. After 72 hours of drug exposure, CellTiter-Glo (Promega) reagent was added and luminescence was measured on a Spectramax spectrophotometer (Molecular Devices, Sunnyvale, CA, USA) according the manufacturer's instructions. Data are presented as percentage of viable cells compared with control cells (vehicle treatment).

Immunoblotting: Cells were washed in PBS and lysed with 25 mM Tris-HCL (pH 7.6), 150 mM NaCl, 1% NP-40, 1% sodium deoxycholate, 0.1% SDS supplemented with Halt Protease Inhibitor Cocktail (Thermo Fisher Scientific) and Halt Phosphatase Inhibitor Cocktail (Thermo Fisher Scientific). Lysates were separated in a 4%–15% SDS-PAGE gel and transferred onto a nitrocellulose membrane (Bio-Rad). Membranes were blocked with 5% fetal bovine serum (FBS) in Tris-buffered saline (TBS) containing 0.1% Tween and incubated with the appropriate antibodies. Detection was performed via ECL Prime (Amersham Biosciences). Antibodies against the following were obtained from Cell Signaling Technology (Danvers, MA, USA) and were used at a dilution of 1:1000: MET (#3148), p-MET Y1349 (#3121), pMEK S217/221 (#9121), ERK1/2 (#3493), p-ERK1/2 T202/Y204 (#9106), HSP90 (#4874), PARP (#9546), horseradish peroxidase (HRP)-conjugated anti-mouse (#7076) and HRP-conjugated anti-rabbit (#7074). The following antibody was obtained from EMD Millipore (Burlington, MA, USA): RAS (05-516, 1:2000 dilution). Detection was performed via ECL Prime (Amersham Biosciences).

Cell-free DNA analysis: Samples were shipped to a Clinical Laboratory Improvement Act (CLIA)-certified, College of American Pathologists–accredited laboratory (Guardant Health, Redwood City, CA). cfDNA was extracted from whole blood collected in 10-mL Streck tubes. After double centrifugation, 5–30 ng of cfDNA was isolated for digital sequencing of either a 70 or 73-gene panel (Supplementary Table 6) as previously described (15). Only those genes in common to these two panels were included in subsequent analysis. Nonsynonymous mutations were further processed with the R statistical computing program (version 3.3). Variants with unknown or neutral predicted functional significance were filtered prior to analysis as previously described (11). Mutations previously reported as associated with clonal

hematopoiesis were also excluded (16). Residue numbering was standardized to MET UniProtKB-P08581.

Next Generation Sequencing: Tumor sample next generation sequencing (NGS) was performed in CLIA-approved laboratories. The Foundation One and Foundation ACT assays are commercially available assays which were used in the clinical standard-of-care setting. The UCSF500 assay sequences 479 cancer-associated genes to target 200X coverage, utilizing sequencing of a PBMC sample, target 100X coverage, as a control. The University of Florida GatorSeq NGS assay, utilized for both tumor tissue and PBMC analysis, performs sequencing of 76 cancer-associated genes with target 500X coverage (Supplemental Table S6). Germline mutations were subtracted utilizing sequencing of buccal swab samples to a target depth of 100X.

Droplet Digital PCR: Isolated genomic DNA extracted from FFPE was amplified using ddPCR Supermix for Probes (Bio-Rad) using KRAS and MET assays (PrimePCR ddPCR Mutation Assay, Bio-Rad, and custom-designed). DNA template (8 µL) was added to 10 µL of ddPCR Supermix for Probes (Bio-Rad) and 2 µL of the primer/ probe mixture. This 20-µL reaction mix was added to a DG8 cartridge together with 70 µL of Droplet Generation Oil for Probes (Bio-Rad) and used for droplet generation. Droplets were then transferred to a 96-well plate (Eppendorf) and then thermal cycled with the following conditions: 5 minutes at 95°C, 40 cycles of 94°C for 30 seconds, 55°C for 1 minute followed by 98°C for 10 minutes (ramp rate 2°C/second). Droplets were analyzed with the QX200 Droplet Reader (Bio-Rad) for fluorescent measurement of FAM and HEX probes. Gating was performed based on positive and negative controls, and mutant populations were identified. The ddPCR data were analyzed with QuantaSoft analysis software (Bio-Rad) to obtain fractional abundance of the mutant DNA alleles in the wild-type (WT)/normal background. The quantification of the target molecule was presented as number of total copies (mutant plus WT) per sample in each reaction. Fractional abundance is calculated as follows: F.A. % = (Nmut/(Nmut + Nwt)) × 100), where Nmut is number of mutant events and Nwt is number of WT events per reaction. Multiple replicates were performed for each sample. ddPCR analysis of normal control genomic DNA (gene fragment obtained from IDT) and no DNA template (water) controls was performed in parallel with all samples, including multiple replicates as contamination-free controls.

Statistical Analysis: Pairwise sample group comparisons for cfDNA analysis were carried out using a two-tailed Fisher's exact t-test, with Benjamini-Hochberg correction for multiple comparisons, using a false discovery rate of <0.2%. For cell viability curves, comparisons were performed using the two-sided student t-test, with significance threshold of p-value < 0.05.

Author contributions

Conception and design: J. Rotow, C. Blakely, T. Bivona

Development of methodology: P. Gui

Acquisition of Data: J. Rotow, V. Raymond, R. Lanman, F. Kaye, N. Peled, F Fece de la Cruz, I Yeh, B. Bastian, P Starostik, K Newsom, V Olivas, B. Nadres, R. Corcoran

Analysis and interpretation of data: J. Rotow, P. Gui, W. Wu, E Collison, C. McCoach, A. Wolff, J. Fraser; Writing, review and or revision of the manuscript: J. Rotow, P. Gui, W. Wu, F. Fece de la Cruz, R. Corcoran, C. Blakely, T. Bivona

Administrative, technical, or material support: V. Raymond, R. Lanman

Tables and Table Legends:

Patient #	Histology	MET TKI Received	New genomic alterations detected after MET TKI Exposure
1	Lung Adenocarcinoma	Crizotinib	*PIK3CA* R38H, *MET* Y1230S, *MET* F1200I, *KRAS* CNG
2	Lung Adenocarcinoma	Crizotinib	*KRAS* G12D[a,b]
3	Lung Adenocarcinoma	Crizotinib	*FBXW7* R689Q, *AR* W742C, *TP53* Y163S, *KIT* CNG
4	Lung Adenocarcinoma	Crizotinib[c]	*CCND1* CNG, *TP53* N239S, *TP53* R248W, *NF1* p.Gln2636fs, *MET* p.Ser244fs
5	Lung Adenocarcinoma	Crizotinib	*AR* CNG, *PIK3CA* CNG, *MET* Y1230H, *MET* D1228N, *EGFR* CNG[b]
		Glesatinib	*MET* L1195V
6	Lung SCC	Crizotinib	*EGFR* CNG, *TP53* p.Arg156del
7	Lung Adenocarcinoma	Crizotinib	None
8	Lung Adenocarcinoma	Crizotinib	*TP53* V173M
9	Lung Adenocarcinoma	Crizotinib	*MET* L1195V, *TP53* V216E, *EGFR* CNG
10	Lung Adenocarcinoma	Crizotinib	None
11	Lung Adenocarcinoma	Crizotinib	*TP53* R158H, *EGFR* R836H, *PDGFRA* R558H
12	NSCLC NOS	Crizotinib	*MET* D1228H, *TP53* F270L[b]

[a]cfDNA analysis via Foundation ACT assay. Sequencing of a tumor biopsy following crizotinib treatment (Foundation One) notable for both *KRAS* G12D and *KRAS* amplification.
[b]Sequencing prior to known MET TKI exposure performed on a tumor biopsy sample rather than via plasma cfDNA analysis, utilizing a University of Florida in-house NGS assay (patient 2), Foundation One (patient 5), or Cancer-Select assay (patient 12).
[c]Followed by pemetrexed prior to cfDNA testing.

Table 1. Acquired gene alterations in the cfDNA of patients treated with a MET TKI. The genomic alterations newly identified upon targeted sequencing for cancer-associated genes in cfDNA samples obtained following known MET TKI exposure compared to results of samples obtained prior to known MET TKI exposure. Sequencing performed via the Guardant 360 assay, unless otherwise specified. Further details for patient one in Figure 2A and further details for patient two in Figure 2B. Additional details regarding patient five have previously been published (6,8). Abbreviations: CNG, copy number gain; NOS, not otherwise specified; SCC, squamous cell carcinoma.

Figures:

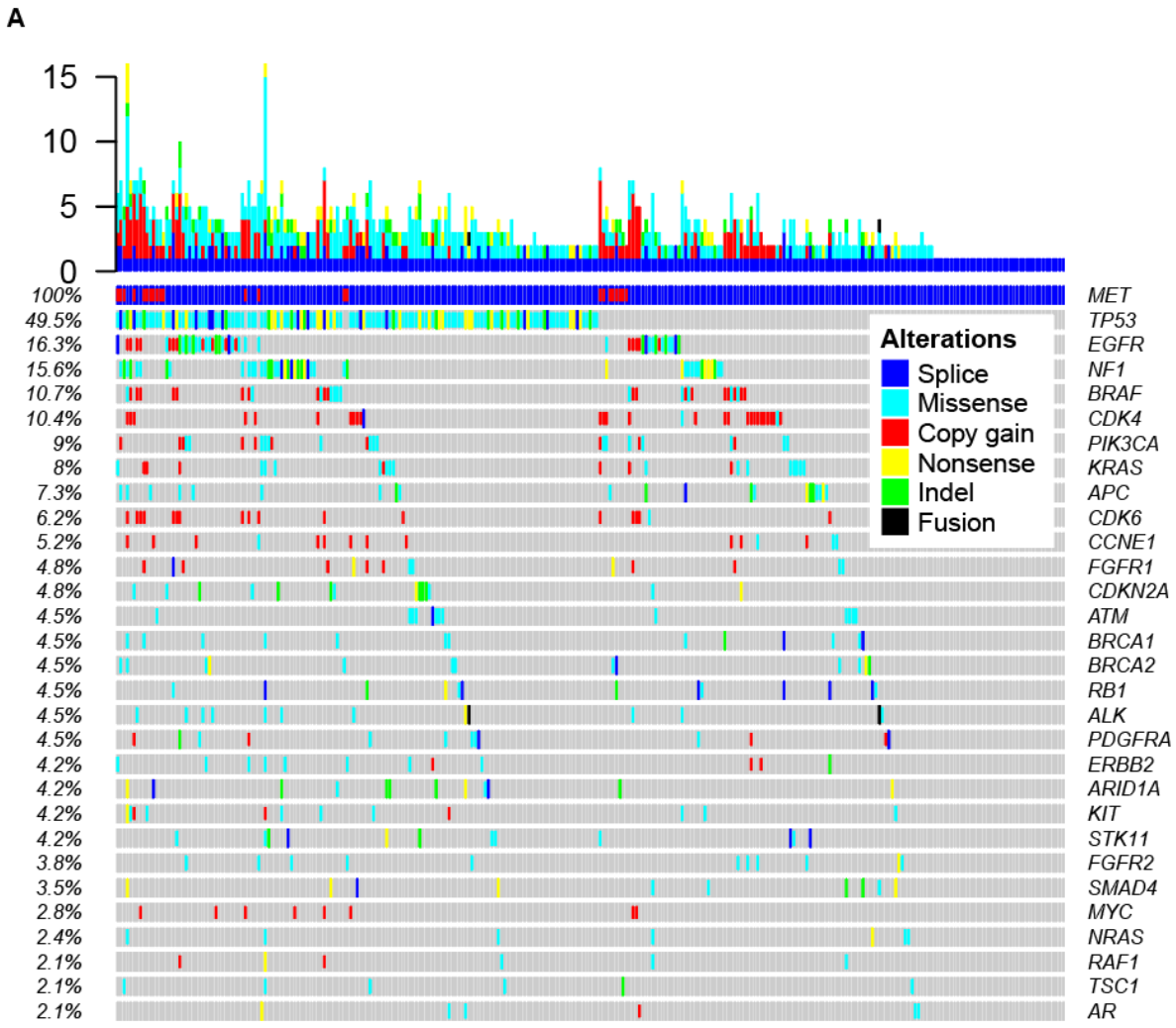

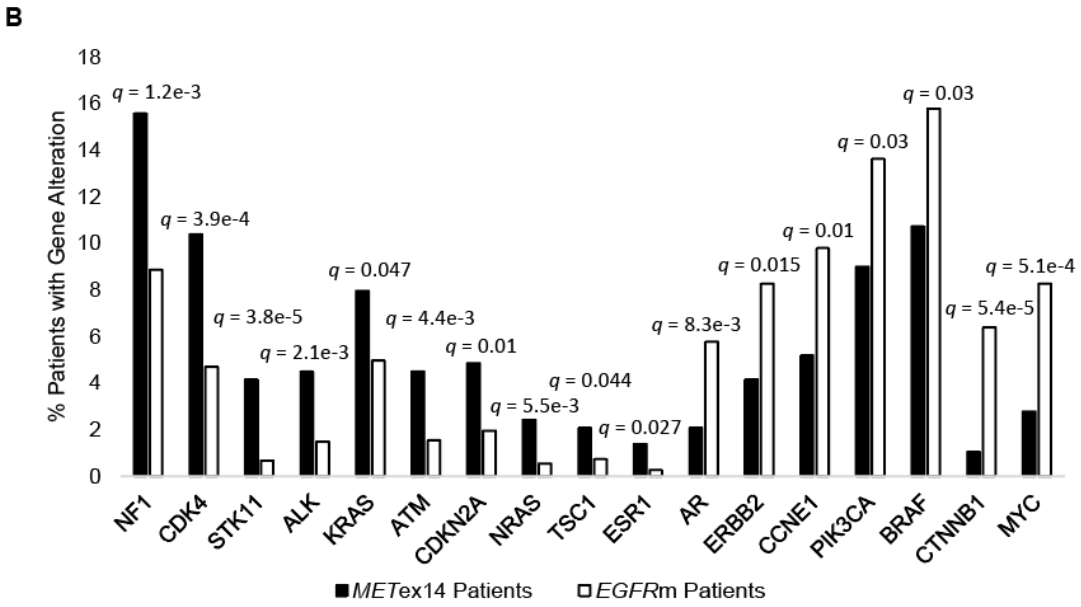

Figure 1. Co-occurring genetic alterations are common in non-small cell lung cancer (NSCLC) with a *MET* exon 14 mutation. A. Distribution of co-occurring genomic alterations in a targeted list of cancer-associated genes (Supplemental Table S6) as detected by cfDNA in 332 samples from 289 patients with advanced-stage *MET*ex14 NSCLC. Results are filtered to exclude synonymous variants, variants predicted to result in an unknown or neutral function impact (via COSMIC v83, GENIE, ClinVar, and mutation assessor prediction algorithms) and mutations previously reported as associated with clonal hematopoiesis. Only genomic alterations occurring at a 2% or greater frequency are displayed. **B.** Comparative frequency of gene alterations in the cohort of advanced-stage *MET*ex14 NSCLC patients (n=289) compared to an independent cohort of patients (n=1489) with a known canonical EGFR activating mutation (EGFR exon 19 deletions, EGFR L858R mutations). Genes with a statistically significant difference (two-tailed Fisher's exact test with Benjamini-Hochberg multiple hypothesis testing for false discovery rate < 0.2) between the two cohorts are displayed.

A

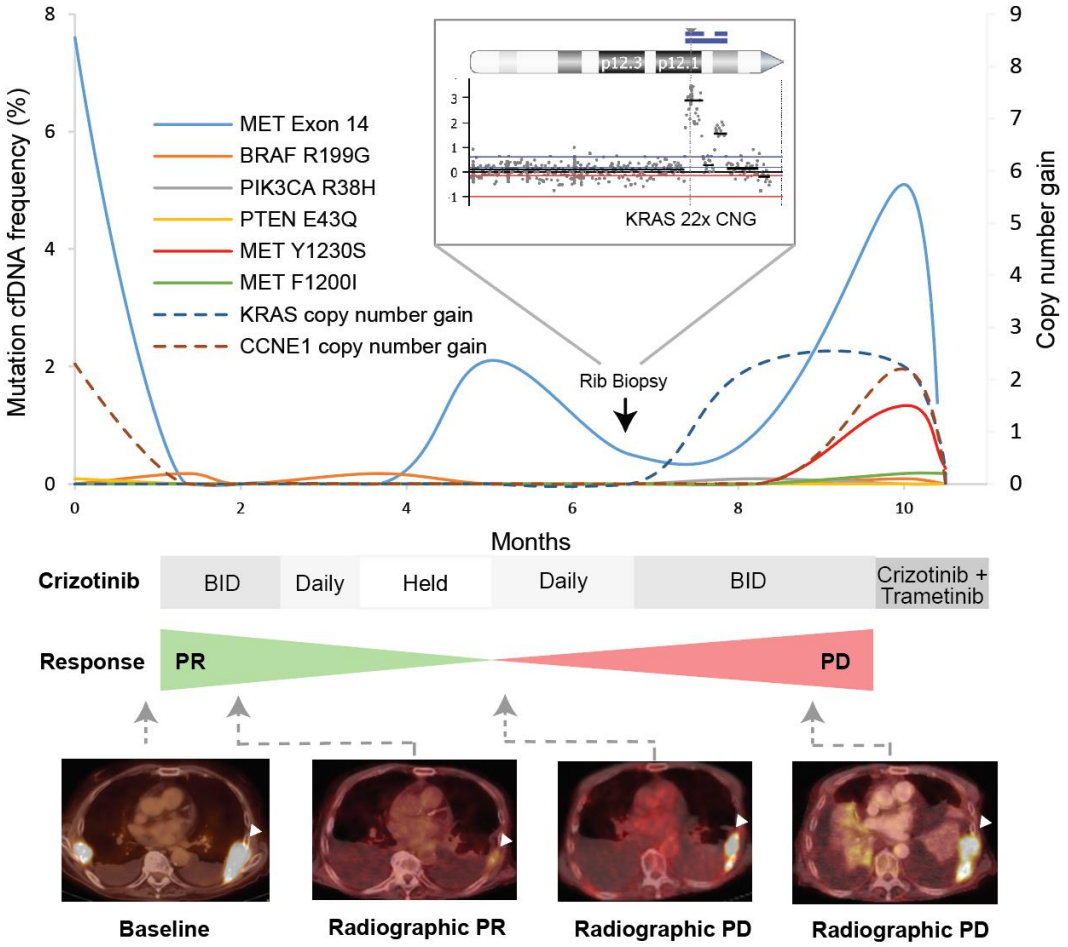

B

	RUL Lung VAF(%)/CNG†	Plasma cfDNA Allele Frequency (%)‡	Abdominal Lesion VAF(%)/CNG*
MET Exon14	8%	2.2%	77.9%
KRAS	Wild type	G12D 7.8%	G12D 47.4%, 11x CNG
ddPCR	METex14 11% KRAS G12D not detected		

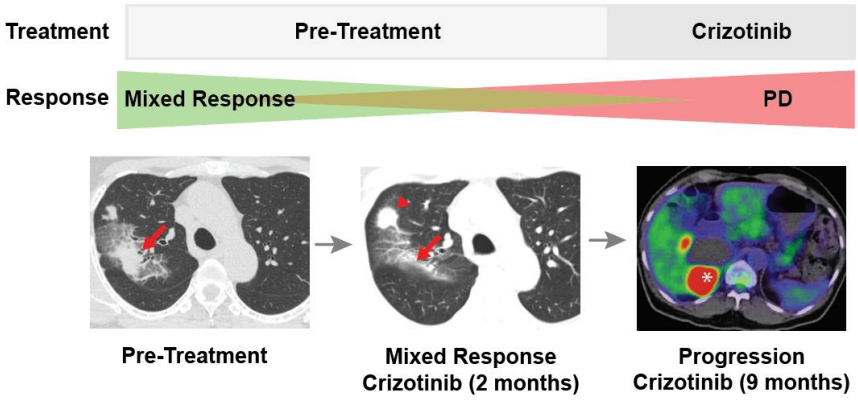

Figure 2. *KRAS* amplification and/or *KRAS G12D* mutation in *MET*ex14 NSCLCs with resistance to crizotinib. **A.** Serial cfDNA analysis for a targeted panel of cancer-associated genes (Supplemental Table S6) in a patient with stage IV MET exon 14 mutated NSCLC, obtained prior to treatment, during partial response to crizotinib and through the development of acquired resistance to crizotinib treatment. The timing of a biopsy of a crizotinib-resistant left-sided metastatic rib lesion, on which a UCSF clinical NGS panel was performed, is shown (black arrow) as are representative PET/CT images, including the sampled left-sided rib metastasis (white arrow head). The inset displays copy number variation at the short arm of chromosome 12 as determined by CNVkit (38) analysis of UCSF500 assay data obtained from a metastatic soft tissue rib lesion, showing 22-fold KRAS amplification. **B.** Serial targeted DNA sequencing of cancer-associated genes performed on tumor tissue samples or plasma cfDNA in a patient with advanced-stage *MET*ex14 NSCLC. DNA sequencing was performed on a pre-treatment biopsy of a lung lesion (red arrow) using a clinical University of Florida gene panel assay and via a commercial plasma cfDNA panel (Foundation ACT) prior to mixed response to crizotinib treatment (response at original lesion, progression at prior small right upper lobe lung lesion highlighted by a red arrowhead), and using the commercial Foundation One panel on a tissue sample of a progressing abdominal lesion (white asterisk) at acquired crizotinib resistance. Key results are shown highlighting a KRAS G12D mutation and acquired KRAS amplification, with full results available in Supplemental Table S5.

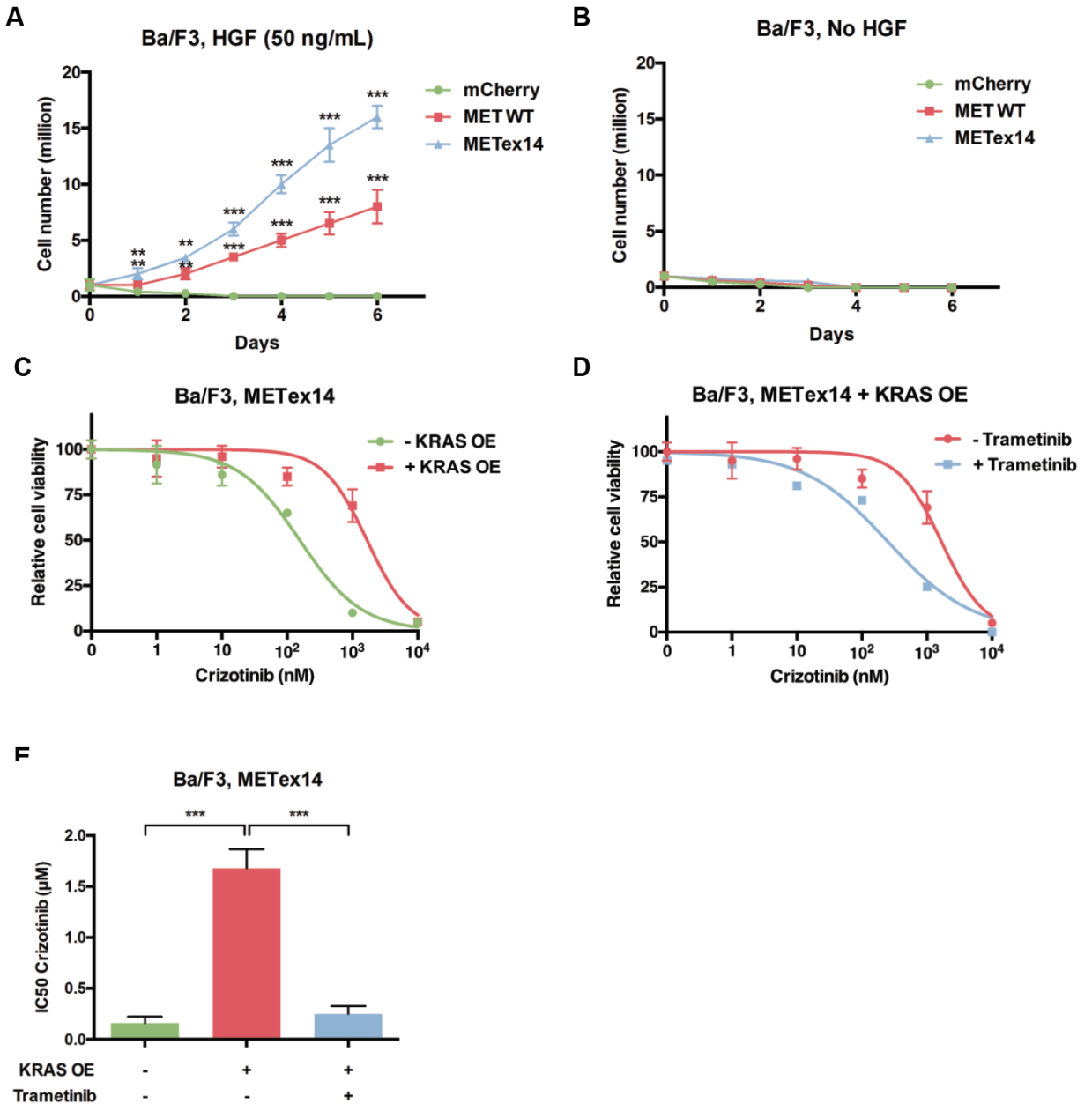

Figure 3. KRAS upregulation promotes MET TKI resistance that is overcome by combined crizotinib and trametinib polytherapy in *MET*ex14 preclinical models. **A.** Ba/F3 cells with wild type MET, METex14, or mCherry control demonstrating acquisition of IL-3 independent growth with addition of HGF (50 ng/mL) in cells expressing the MET exon 14 mutant and to a lesser extent in cells expressing wild type MET. **B.** Cell growth curves of Ba/F3 cells expressing wild type MET, METex14, or mCherry control without growth in the absence of IL-3 and HGF. **C.** Cell viability curves demonstrating a shift in the half maximal inhibitory concentration (IC50) to crizotinib with overexpression of wild type KRAS in MET exon 14-mutant expressing Ba/F3 cells. The cells were grown in culture with HGF supplementation (50 ng/mL). **D.** Cell viability curve for crizotinib treatment in Ba/F3 cells with both METex14 expression and wild type KRAS overexpression (KRAS OE), in the setting of treatment with trametinib at 0.01 μM and supplementation with HGF 50 ng/mL, showing decrease in the IC50 to crizotinib when used in

combination with trametinib. The KRAS OE, trametinib negative curves in panel C and D reflect the same experimental data, displayed on two graphs for clarity. **E.** Summary graph of IC50 to crizotinib with and without KRAS overexpression and/or trametinib treatment. ** *p*-value < 0.01, *** *p*-value < 0.001 by student's t-test.

References:

1. Frampton GM, Ali SM, Rosenzweig M, Chmielecki J, Lu X, Bauer TM*, et al.* Activation of MET via diverse exon 14 splicing alterations occurs in multiple tumor types and confers clinical sensitivity to MET inhibitors. Cancer Discov 2015;5(8):850-9.
2. Comprehensive molecular profiling of lung adenocarcinoma. Nature 2014;511(7511):543-50.
3. Paik PK, Drilon A, Fan PD, Yu H, Rekhtman N, Ginsberg MS*, et al.* Response to MET inhibitors in patients with stage IV lung adenocarcinomas harboring MET mutations causing exon 14 skipping. Cancer Discov 2015;5(8):842-9.
4. Drilon AE, Camidge DR, Ou SH, Clark J, Socinski MA, Weiss J*, et al.* Efficacy and safety of crizotinib in patients (pts) with advanced MET exon 14-altered non-small cell lung cancer (NSCLC). J Clin Oncol 2016;34(Suppl; abstract 108).
5. Awad MM, Leonardi GC, Kravets S, Dahlberg SE, Drilon AE, Noonan S. Impact of MET inhibitors on survival among patients (pts) with *MET* exon 14 mutant (*MET*del14) non-small cell lung cancer (NSCLC). J Clin Oncol 2017;35(supple; abstract 8511).
6. Engstrom LD, Aranda R, Lee M, Tovar EA, Essenburg CJ, Madaj Z*, et al.* Glesatinib Exhibits Antitumor Activity in Lung Cancer Models and Patients Harboring MET Exon 14 Mutations and Overcomes Mutation-mediated Resistance to Type I MET Inhibitors in Nonclinical Models. Clin Cancer Res 2017;23(21):6661-72.
7. Bahcall M, Sim T, Paweletz CP, Patel JD, Alden RS, Kuang Y*, et al.* Acquired METD1228V Mutation and Resistance to MET Inhibition in Lung Cancer. Cancer Discov 2016;6(12):1334-41.
8. Lu X, Peled N, Greer J, Wu W, Choi P, Berger AH*, et al.* MET Exon 14 Mutation Encodes an Actionable Therapeutic Target in Lung Adenocarcinoma. Cancer Res 2017;77(16):4498-505.
9. Rotow J, Bivona TG. Understanding and targeting resistance mechanisms in NSCLC. Nat Rev Cancer 2017;17(11):637-58.
10. Trusolino L, Bertotti A, Comoglio PM. MET signalling: principles and functions in development, organ regeneration and cancer. Nat Rev Mol Cell Biol 2010;11(12):834-48.
11. Blakely CM, Watkins TBK, Wu W, Gini B, Chabon JJ, McCoach CE*, et al.* Evolution and clinical impact of co-occurring genetic alterations in advanced-stage EGFR-mutant lung cancers. Nat Genet 2017;49(12):1693-704.
12. Jordan EJ, Kim HR, Arcila ME, Barron D, Chakravarty D, Gao J*, et al.* Prospective Comprehensive Molecular Characterization of Lung Adenocarcinomas for Efficient Patient Matching to Approved and Emerging Therapies. Cancer Discov 2017;7(6):596-609.
13. McCoach CE, Blakely CM, Banks KC, Levy B, Chue BM, Raymond VM*, et al.* Clinical Utility of Cell-Free DNA for the Detection of ALK Fusions and Genomic Mechanisms of ALK Inhibitor Resistance in Non-Small Cell Lung Cancer. Clin Cancer Res 2018;24(12):2758-70.
14. Russo M, Siravegna G, Blaszkowsky LS, Corti G, Crisafulli G, Ahronian LG*, et al.* Tumor Heterogeneity and Lesion-Specific Response to Targeted Therapy in Colorectal Cancer. Cancer Discov 2016;6(2):147-53.
15. Odegaard JI, Vincent JJ, Mortimer S, Vowles JV, Ulrich BC, Banks KC*, et al.* Validation of a Plasma-Based Comprehensive Cancer Genotyping Assay Utilizing Orthogonal Tissue- and Plasma-Based Methodologies. Clin Cancer Res 2018.

16. Ptashkin RN, Mandelker DL, Coombs CC, Bolton K, Yelskaya Z, Hyman DM, *et al.* Prevalence of Clonal Hematopoiesis Mutations in Tumor-Only Clinical Genomic Profiling of Solid Tumors. JAMA Oncol 2018.
17. Heist RS, Sequist LV, Borger D, Gainor JF, Arellano RS, Le LP, *et al.* Acquired Resistance to Crizotinib in NSCLC with MET Exon 14 Skipping. J Thorac Oncol 2016;11(8):1242-5.
18. Ou SI, Young L, Schrock AB, Johnson A, Klempner SJ, Zhu VW, *et al.* Emergence of Preexisting MET Y1230C Mutation as a Resistance Mechanism to Crizotinib in NSCLC with MET Exon 14 Skipping. J Thorac Oncol 2017;12(1):137-40.
19. Schrock AB, Lai A, Ali SM, Miller VA, Raez LE. Mutation of MET Y1230 as an Acquired Mechanism of Crizotinib Resistance in NSCLC with MET Exon 14 Skipping. J Thorac Oncol 2017;12(7):e89-e90.
20. Schmidt L, Junker K, Nakaigawa N, Kinjerski T, Weirich G, Miller M, *et al.* Novel mutations of the MET proto-oncogene in papillary renal carcinomas. Oncogene 1999;18(14):2343-50.
21. Katayama R, Shaw AT, Khan TM, Mino-Kenudson M, Solomon BJ, Halmos B, *et al.* Mechanisms of acquired crizotinib resistance in ALK-rearranged lung Cancers. Sci Transl Med 2012;4(120):120ra17.
22. Goode B, Mondal G, Hyun M, Ruiz DG, Lin YH, Van Ziffle J, *et al.* A recurrent kinase domain mutation in PRKCA defines chordoid glioma of the third ventricle. Nat Commun 2018;9(1):810.
23. Mandanas RA, Boswell HS, Lu L, Leibowitz D. BCR/ABL confers growth factor independence upon a murine myeloid cell line. Leukemia 1992;6(8):796-800.
24. Greulich H, Chen TH, Feng W, Janne PA, Alvarez JV, Zappaterra M, *et al.* Oncogenic transformation by inhibitor-sensitive and -resistant EGFR mutants. PLoS Med 2005;2(11):e313.
25. Reungwetwattana T, Liang Y, Zhu V, Ou SI. The race to target MET exon 14 skipping alterations in non-small cell lung cancer: The Why, the How, the Who, the Unknown, and the Inevitable. Lung Cancer 2017;103:27-37.
26. Hrustanovic G, Olivas V, Pazarentzos E, Tulpule A, Asthana S, Blakely CM, *et al.* RAS-MAPK dependence underlies a rational polytherapy strategy in EML4-ALK-positive lung cancer. Nat Med 2015;21(9):1038-47.
27. Crystal AS, Shaw AT, Sequist LV, Friboulet L, Niederst MJ, Lockerman EL, *et al.* Patient-derived models of acquired resistance can identify effective drug combinations for cancer. Science 2014;346(6216):1480-6.
28. Zhu YC, Lin XP, Li XF, Wu LX, Chen HF, Wang WX, *et al.* Concurrent ROS1 gene rearrangement and KRAS mutation in lung adenocarcinoma: A case report and literature review. Thorac Cancer 2018;9(1):159-63.
29. Cargnelutti M, Corso S, Pergolizzi M, Mevellec L, Aisner DL, Dziadziuszko R, *et al.* Activation of RAS family members confers resistance to ROS1 targeting drugs. Oncotarget 2015;6(7):5182-94.
30. Ohashi K, Sequist LV, Arcila ME, Moran T, Chmielecki J, Lin YL, *et al.* Lung cancers with acquired resistance to EGFR inhibitors occasionally harbor BRAF gene mutations but lack mutations in KRAS, NRAS, or MEK1. Proc Natl Acad Sci U S A 2012;109(31):E2127-33.
31. de Bruin EC, Cowell C, Warne PH, Jiang M, Saunders RE, Melnick MA, *et al.* Reduced NF1 expression confers resistance to EGFR inhibition in lung cancer. Cancer Discov 2014;4(5):606-19.
32. Tricker EM, Xu C, Uddin S, Capelletti M, Ercan D, Ogino A, *et al.* Combined EGFR/MEK Inhibition Prevents the Emergence of Resistance in EGFR mutant Lung Cancer. Cancer Discov 2015.
33. Ercan D, Xu C, Yanagita M, Monast CS, Pratilas CA, Montero J, *et al.* Reactivation of ERK signaling causes resistance to EGFR kinase inhibitors. Cancer Discov 2012;2(10):934-47.
34. Ho CC, Liao WY, Lin CA, Shih JY, Yu CJ, Chih-Hsin Yang J. Acquired BRAF V600E Mutation as Resistant Mechanism after Treatment with Osimertinib. J Thorac Oncol 2017;12(3):567-72.
35. Janne PA, van den Heuvel MM, Barlesi F, Cobo M, Mazieres J, Crino L, *et al.* Selumetinib Plus Docetaxel Compared With Docetaxel Alone and Progression-Free Survival in Patients With KRAS-

Mutant Advanced Non-Small Cell Lung Cancer: The SELECT-1 Randomized Clinical Trial. Jama 2017;317(18):1844-53.

36. Awad MM, Oxnard GR, Jackman DM, Savukoski DO, Hall D, Shivdasani P*, et al.* MET Exon 14 Mutations in Non-Small-Cell Lung Cancer Are Associated With Advanced Age and Stage-Dependent MET Genomic Amplification and c-Met Overexpression. J Clin Oncol 2016;34(7):721-30.
37. Hu Y, Ulrich B, Supplee J, Kuang Y, Lizotte PH, Feeney N*, et al.* False positive plasma genotyping due to clonal hematopoiesis. Clin Cancer Res 2018.
38. Talevich E, Shain AH, Botton T, Bastian BC. CNVkit: Genome-Wide Copy Number Detection and Visualization from Targeted DNA Sequencing. PLoS Comput Biol 2016;12(4):e1004873.